CALT-68-1311
DOE RESEARCH AND
DEVELOPMENT REPORT
UTPT-85-37

Quark Model Predictions for the Electron Energy Spectrum in Semileptonic D and B Decays*

Benjamin Grinstein[f1] and Mark B. Wise[f2]
California Institute of Technology, Pasadena, CA 91125

Nathan Isgur
Department of Physics, University of Toronto, Toronto, Canada M5S 1A7

ABSTRACT

The constituent quark model is used to predict the electron energy spectrum in semileptonic D and B meson decays. Particular attention is paid to the endpoint region of the electron spectrum in B decays since this is crucial to a determination of the $b \to u$ weak mixing angle.

January 7, 1986

[f1] Tolman Research Fellow
[f2] Alfred P. Sloan Foundation Fellow and U.S. Department of Energy Outstanding Junior Investigator Program under Contract No. DE-FG03-84ER40172.

I. Introduction

In the standard model, based on the gauge group SU(3) × SU(2) × U(1), the quarks couple to the W−bosons through the weak current

$$J^{\mu} = \frac{g_2}{2\sqrt{2}} \bar{u}_i \gamma^{\mu}(1 - \gamma_5) V_{ij} d_j \equiv \frac{g_2}{2\sqrt{2}} V_{ij} j_{ij}^{\mu} . \tag{1}$$

In eq. (1) $i, j \in \{1, \cdots, n\}$ are generation indices and V_{ij} is an $n \times n$ unitary matrix that arises from diagonalization of the quark mass matrices. At present there is experimental evidence for three generations of quarks and leptons. In this case it is possible, by redefining the phases of quark fields, to write V in terms of three angles θ_1, θ_2, θ_3 and a phase δ (ref. 1)

$$V = \begin{pmatrix} c_1 & -s_1 c_3 & -s_1 s_3 \\ s_1 c_2 & c_1 c_2 c_3 - s_2 s_3 e^{i\delta} & c_1 c_2 s_3 + s_2 c_3 e^{i\delta} \\ s_1 s_2 & c_1 s_2 c_3 + c_2 s_3 e^{i\delta} & c_1 s_2 s_3 - c_2 c_3 e^{i\delta} \end{pmatrix} . \tag{2}$$

Here $c_i \equiv \cos\theta_i$, $s_i \equiv \sin\theta_i$ and the angles θ_i are chosen to lie in the first quadrant.

In the standard model the elements of the matrix V_{ij} are fundamental parameters, and their values must be determined experimentally. Experimental information on θ_1 comes from nuclear β−decay and semileptonic hyperon decays. Experimental information on the angles θ_2 and θ_3 can be obtained from semileptonic B−meson decays. The differential rate for semileptonic B−meson decay has the form ($V_{13} \equiv V_{ub}$ and $V_{23} \equiv V_{cb}$)

$$d\Gamma(B \to e\bar{\nu}X) = |V_{cb}|^2 d\hat{\Gamma}(B \to X_c e\bar{\nu}) + |V_{ub}|^2 d\hat{\Gamma}(B \to X_u e\bar{\nu}) , \tag{3}$$

where $d\hat{\Gamma}(B \to X_q e\bar{\nu})$ denotes the contributions to $d\Gamma(B \to X e\bar{\nu})$ from the part

of the weak current (excluding the weak mixing angles) where a bottom quark couples to a quark $q = c$ or u. In the free quark model where the bottom quark decays freely from rest

$$\hat{\Gamma}(B \to X_q e\bar{\nu}) = \frac{G_F^2 m_b^5}{192\pi^3} f(m_q/m_b) \tag{4}$$

where $f(x) = 1 - 8x + 8x^6 - x^8 - 24x^4 \ln x$.

The contribution to $\Gamma(B \to X\, e\bar{\nu})$ coming from the $b \to u$ coupling can, in principle, be isolated experimentally by examining semileptonic B decays with electron energies that are so large that the mass of the hadronic state X must be less than the D meson mass. However, this endpoint of the electron energy spectrum comes from the production of a few low mass hadronic resonances and is sensitive to nonperturbative strong interaction effects, so that it cannot be satisfactorily treated in the free quark model. To treat this region of the spectrum requires a method for explicitly summing over low mass states X_c and X_u to predict the shapes and strengths of both spectra in the endpoint region. Unfortunately, although perturbative QCD can be used to predict the total rates with reasonable reliability, there are no rigorous methods available at the moment for handling these non-perturbative QCD effects which are crucial to determining the $b \to u$ coupling. Until such methods become available, we must therefore rely on models of the low-lying hadrons to predict the endpoint spectrum we need.

The quark model is a phenomenological model of QCD in the non-perturbative regime which has had considerable success in describing hadronic structure.[2] It is especially well suited (and well tested) for describing the low-lying hadrons which one needs to predict the $B \to X\, e\bar{\nu}$ endpoint spectrum. The main purpose of this paper is to apply the quark model to this problem. The

calculations which we present here are based on the use of the non–relativistic version of the quark potential model; possible improvements on this simplest model will be discussed in our concluding section.

II. Method

The transition matrix element for the process $B^{(-)}_{(0)} \to X^{(+)}_{(0)}_q e^- \overline{\nu}_e$ is

$$T = \frac{G_F}{\sqrt{2}} V_{qb}\, \overline{u}_e \gamma_\mu (1 - \gamma_5)\, v_{\nu_e} \left\langle X_q(p_X s_X) \,\middle|\, j^\mu_{qb} \,\middle|\, B(p_B) \right\rangle , \tag{5}$$

where V_{qb} is the element of the Kobayashi–Maskawa matrix (2) appropriate for the $B \to X_q$ transition and j^μ_{qb} is the charged hadronic current in (1). Since the hadronic tensor

$$h_{\mu\nu} \equiv \sum_{s_X} \left\langle B(p_B) \,\middle|\, j^\dagger_\nu \,\middle|\, X(p_X s_X) \right\rangle \left\langle X(p_X s_X) \,\middle|\, j_\mu \,\middle|\, B(p_B) \right\rangle , \tag{6}$$

must have the form

$$\begin{aligned} h_{\mu\nu} = &- \alpha\, g_{\mu\nu} + \beta_{++}(p_B + p_X)_\mu (p_B + p_X)_\nu + \beta_{+-}(p_B + p_X)_\mu (p_B - p_X)_\nu \\ &+ \beta_{-+}(p_B - p_X)_\mu (p_B + p_X)_\nu + \beta_{--}(p_B - p_X)_\mu (p_B - p_X)_\nu \\ &+ i\gamma\, \varepsilon_{\mu\nu\rho\sigma} (p_B + p_X)^\rho (p_B - p_X)^\sigma . \end{aligned} \tag{7}$$

one can easily show, if the mass of the electron is neglected, that the differential decay rate of the B meson depends only on α, β_{++}, and γ and is given by

$$\frac{d^2\Gamma}{dx\,dy} = |V_{qb}|^2 \frac{G_F^2 m_B^5}{32\pi^3}\left\{\frac{\alpha}{m_B^2}y + 2\beta_{++}[2x(1-\frac{m_X^2}{m_B^2}+y) - 4x^2 - y]\right.$$

$$\left. - \gamma y[1 - \frac{m_X^2}{m_B^2} - 4x + y]\right\}, \tag{8}$$

where $x \equiv \frac{E_e}{m_B}$ and $y \equiv \frac{t}{m_B^2} = \frac{(p_B - p_X)^2}{m_B^2}$. Of course the result eq. (8) holds for other $M \to M' e^- \bar{\nu}_e$ decays with the appropriate substitutions; for decays to $e^+ \nu_e$ one must in addition reverse the sign of the term proportional to γ.

As explained in the introduction, we will estimate α, β_{++}, and γ (for each channel X) using the quark model, building up the total electron spectrum $\frac{d\Gamma}{dx}$ by summing over contributing states X. If we include states X with mass up to m_X, we will then have the complete spectrum from the maximum value of x down to $x = \frac{1}{2}(1 - \frac{m_X^2}{m_B^2})$ so that this method – in contrast to a free quark calculation – is very suitable for studying the crucial endpoint region of the spectrum.

Central to this calculation is, obviously, the possibility of reliably estimating the matrix elements $\langle X | j^\mu | B \rangle$ and the inclusion of all relevant states which will contribute above some minimum x. Our first assumption is that we can work in the approximation where we ignore the creation of additional quark–antiquark pairs. This means that the sum over final hadronic states X will be saturated by $q\bar{q}$ states, and that these states can be treated in the zero–width limit. (The widths of the $q\bar{q}$ states, which we are assuming to be responsible for populating multihadron channels, could be included in a straightforward way, but we expect that this detail would have very minor effects on $\frac{d\Gamma}{dx}$.) One might at this point

conclude that it would be sufficient to sum over only the $q\bar{q}$ states of the usual quark model. For sufficiently small m_X this should be true, but for large m_X one must expect contributions from gluonic excitations of mesons (hybrid mesons). While in principle we could include such states in our calculation, this observation along with the sheer complexity of extending the sum over X to very high m_X will mean that in practice we will truncate our sums at some maximum m_X.

With these approximations we have reduced our problem to that of calculating the matrix elements $\langle X | j^\mu | B \rangle$ for the low-lying ordinary mesonic resonances; it is natural to use the constituent quark model to make such a calculation. Since the major uncertainties in our results will arise from our use of the quark model to estimate these matrix elements, we will thoroughly describe our procedure in this section. In a subsequent section we will describe the evidence from various sources which bear on the reliability of these procedures.

The basic idea of our method[3,4] is to make a correspondence between the Lorentz invariant form factors f which occur in the expansion of the matrix element $\langle X(p_X, s_X) | j^\mu | B(p_B) \rangle$ of the physical B and X and those (which we call $\tilde{f}$) which appear in the quark model calculation $\langle \tilde{X}(\tilde{p}_X \tilde{s}_X) | j^\mu | \tilde{B}(\tilde{p}_B) \rangle$ (where, e.g., $|\tilde{B}(\tilde{p}_B)\rangle$ is the quark model state vector in the weak binding, non-relativistic limit). Form factors $\tilde{f}$ which appear in terms that are of sufficiently low order in momenta can be calculated in this limit. The corresponding form factors f are taken to match onto $\tilde{f}$ at the zero recoil point; higher order form factors are neglected.

As an example, consider the matrix element for $B^0 \to D^+$, where D^+ is the $c\bar{d}$ pseudoscalar ground state meson. In general

$$\langle D^+(p_D)\,|\,j_{c\bar{b}}^{\mu}\,|\,B^0(p_B)\rangle = f_+(p_B + p_D)^{\mu} + f_-(p_B - p_D)^{\mu}\,, \tag{9}$$

where $f_\pm$ are Lorentz invariant form factors which can be considered as functions of $t - t_m$ where $t_m = (m_B - m_D)^2$. (Note that in this example $\alpha = 0$, $\beta_{++} = |f_+|^2$, and $\gamma = 0$ so that in fact only the f_+ form factor is really required.) In the weak binding, non–relativistic limit, the matrix element of $j_{c\bar{b}}^{\mu}$ between quark model states $\tilde{B}^0(\tilde{p}_B)$ and $\tilde{D}^+(\tilde{p}_D)$ [with, e.g., $\tilde{m}_B = m_b + m_d$ so that $\tilde{E}_B = (\tilde{m}_B^2 + \vec{p}_B^{\,2})^{\frac{1}{2}}$] has an expansion exactly analogous to eq. (9) with form factors $\tilde{f}_\pm$ that are functions of $\tilde{t} - \tilde{t}_m$. Our prescription is to take $f_\pm(t - t_m) = \tilde{f}_\pm(t - t_m)$. Since t_m is the value of t for $\vec{p}_B = \vec{p}_D = 0$, this gives the usual quark model correspondence between $f_\pm$ and $\tilde{f}_\pm$ at zero recoil.

The calculation of the form factors $\tilde{f}$ is straightforward. In the weak–binding, non–relativistic limit the properly normalized meson state vectors have the form

$$|X(p_X s_X)\rangle = \sqrt{2\tilde{m}_X}\int d^3p \sum C^{s_x L\, S}_{m_L m_s}\,\phi_X(\vec{p})_{Lm_L}\chi^{Sm_*}_{s\bar{s}}$$

$$\cdot\ |\ q(\frac{m_q}{\tilde{m}_X}\vec{p}_X + \vec{p}, s)\bar{q}(\frac{m_{\bar{q}}}{\tilde{m}_X}\vec{p}_X - \vec{p}, \bar{s})\rangle \tag{10}$$

where $\chi^{Sm_*}_{s\bar{s}}$ couples the spins s and $\bar{s}$ to the spin S, $\phi_X(\vec{p})_{Lm_L}$ is the $q\,\bar{q}$ relative momentum wavefunction, and the C–factors couple L and S to the total spin s_X. This form is correct to leading order in v/c. Ignoring strong renormalization of the weak currents from calculating at the constituent quark scale ($\sim 1\,GeV$), one then simply computes free quark matrix elements between states $\tilde{B}$ and $\tilde{X}$ of the form (10). In our example one easily finds that

$$(\tilde{m}_B + \tilde{m}_D)\tilde{f}_+ + (\tilde{m}_B - \tilde{m}_D)\tilde{f}_- = (4\tilde{m}_B\tilde{m}_D)^{1/2}\int d^3p\,\phi_D^*(\vec{p} + \frac{m_d}{\tilde{m}_D}\vec{p}_D)\phi_B(\vec{p}) \tag{11}$$

$$(\tilde{f}_+ - \tilde{f}_-)\vec{p}_D = (4\tilde{m}_B\tilde{m}_D)^{1/2}\int d^3p\,\phi_D^*(\vec{p} + \frac{m_d}{\tilde{m}_D}\vec{p}_D)\phi_B(\vec{p})[\frac{\vec{p}}{2m_b} + \frac{\vec{p}+\vec{p}_D}{2m_q}]\,, \tag{12}$$

for $\vec{p}_B = 0$ and $\vec{p}_D \ll \tilde{m}_D$. To proceed much further, one in general requires explicit momentum wavefunctions. We have chosen to use Schrödinger wavefunctions appropriate to the usual Coulomb plus linear potential

$$V(r) = -\frac{4\alpha_s}{3r} + c + br \tag{13}$$

with $\alpha_s = 0.5$, $c = -0.84\,GeV$, and $b = 0.18\,GeV^2$, and with constituent quark masses $m_u = m_d = 0.33\,GeV$, $m_s = 0.55\,GeV$, $m_c = 1.82\,GeV$, and $m_b = 5.12\,GeV$. This simple model gives quite reasonable spin–averaged spectra of $u\bar{d}$, $c\bar{d}$, and $b\bar{d}$ mesons up to $L = 2$, and extends satisfactorily to the $c\bar{c}$ and $b\bar{b}$ systems (where we do not need it) with a running $\alpha_s = 0.4$ and 0.3, respectively. To avoid extensive numerical calculations, we use variational solutions of this Schrödinger problem based on harmonic oscillator wavefunctions:

$$\psi^{1S} = \frac{\beta_S^{3/2}}{\pi^{3/4}}e^{-\frac{1}{2}\beta_S^2 r^2} \tag{14}$$

$$\psi_{11}^{1P} = -\frac{\beta_P^{5/2}}{\pi^{3/4}}r_+ e^{\frac{-1}{2}\beta_P^2 r^2} \tag{15}$$

$$\psi^{2S} = \sqrt{\frac{2}{3}}\frac{\beta_S^{7/2}}{\pi^{3/4}}(r^2 - \frac{3}{2}\beta_S^{-2})e^{\frac{-1}{2}\beta_S^2 r^2}\,, \tag{16}$$

in which the β's are employed as variational parameters. The resulting β values are given in Table I. With these wavefunctions we can perform all the integrals we encounter analytically. The formulas for α, β_{++}, and γ for the mesons with $1S$, $1P$, and $2S$ spatial wavefunctions are given in the Appendix. These formulas can be used to calculate $\frac{d\Gamma}{dx}$. Before doing so, however, we must address a generic problem of our non–relativistic calculation. The reader may already have wondered how we can, for example, calculate the slopes of form factors, since such slopes appear in terms of order $\vec{p}_X^{\,2}$ and so may contain contributions from relativistic effects. Indeed, the answer is that the effective radii r_f of our form factors ($f(\vec{p}_X^{\,2}) \equiv 1 - \frac{1}{6} r_f^2 \, \vec{p}_X^{\,2} + \cdots$) include only wavefunction overlap effects and so can be in error by terms of order $1/m_q$. In a truly non–relativistic situation $1/m_q \ll r_f$ so that such corrections are unimportant, but in the cases at hand we are not surprised to find that our calculated pion and kaon charge radii are about 30% below their experimental values. (Meson charge form factors follow as special cases of (11) and (12).) We have therefore compensated all of our effective radii by this amount to produce our best estimates of semileptonic decay rates. With a few exceptions, to be discussed below, whether or not this defect is corrected is of little importance.

III. Results

In this section we will present our results not only for B decay, but also for related processes like $K \to \pi \, e^- \bar{\nu}_e$ and $D \to X \, e^+ \nu_e$ since in the cases where data exists it supports the applicability of our methods. In the next section we will explain why we believe our results are the most reliable available at present, their limitations, and the possibilities for improving them.

a) $K \to \pi e^- \overline{\nu}_e$

This process was studied previously[3] by the methods used here. We also find $f_+(t_m) \simeq 1.02$ and $f_-(t_m) \simeq -0.29$, both of which are in good agreement with experiment. We also agree with the measured t–dependence of the form factor f_+. Note that although SU(3) breaking in the quark masses is substantial, the Ademollo–Gatto theorem[5] continues to protect f_+ from substantial deviations from unity.

b) $D \to X e^+ \nu_e$

All strange mesons X with masses $m_X < m_D$ can contribute to the electron spectrum for D meson decay. Figure 1 shows our full predicted spectrum and how it is built up from contributing resonances. The free quark decay spectrum is shown for comparison. Note that our spectrum is dominated by the two processes $D \to K e^+ \nu_e$ and $D \to K^* e^+ \nu_e$ which we predict to constitute approximately 40% and 58% of the total respectively. This saturation by K and K^* is in agreement with experiment[6,7], which gives for the ratio $K/(K+K^*)$ the value $50 \pm 11\%$; our $D \to K$ form factor is also in agreement with the measured form factor[6]. Finally, we note that our *absolute* prediction for the total rate for semileptonic D decay is $\Gamma(D^0 \to X e^+ \nu_e) = \Gamma(D^+ \to X e^+ \nu_e) = 0.21 \times 10^{12} sec^{-1}$, in reasonable agreement with the experimental result[6,7] of $(0.19 \pm .02) \times 10^{12}\,\mathrm{sec}^{-1}$. Figure 2 shows our predicted electron spectrum, boosted as is appropriate for $D\overline{D}$ pairs produced from the $\psi(3770)$, compared to an experimental spectrum[8] of such electrons. Our model thus clearly gives an account of these decays which seems to be accurate to about 20%. Fig. 3 shows our predictions for the electron spectra from Cabibbo suppressed D^0 decays. The spectrum is dominated by the two processes $D^0 \to \pi^- e^+ \nu_e$ and $D^0 \to \rho^- e^+ \nu_e$ which constitute about 33% and 61% of the total respectively. We will discuss the

interest of these processes in our concluding section.

c) $B \to X\, e^- \bar{\nu}_e$

We now turn to the cases of interest for extracting $|V_{ub}|^2/|V_{cb}|^2$. We first discuss $B \to X_c\, e^- \bar{\nu}_e$ where X_c is a charmed meson with mass $m_X < m_B$. Our present calculations extend only up to $m_X \simeq 2.5\, GeV$, but as can be seen from Fig. 4, which shows how our predicted spectrum is built up out of contributing resonances, the full rate appears to be rapidly saturated by the lowest–lying states. We show the free quark decay spectrum for comparison: note that our spectrum is softer in the endpoint region. Our spectrum is once again dominated by the 1^1S_0 and 1^3S_1 states with the $D(1.87)$ and $D^*(2.02)$ contributing 19% and 71% (respectively) of our total spectrum. This $D^*/(D + D^*)$ ratio of 0.79 is in good agreement with the preliminary experimental measurements [7,9] of 0.85 ± 0.32.

Anticipating that $b \to u / b \to c$ will be small, our *absolute prediction* for the total B semileptonic rate is

$$\Gamma(B^0 \to X^+ e^- \bar{\nu}_e) = \Gamma(B^- \to X^0 e^- \bar{\nu}_e) = 0.58 \times 10^{14} sec^{-1} |V_{cb}|^2 . \qquad (17)$$

From the experimental value of this rate[7] we find that

$$|V_{cb}| = .041 \pm .004 \pm .005 . \qquad (18)$$

We will discuss the uncertainties in this determination of $|V_{cb}|$ associated with our calculation(the second error in (18); the first is experimental and arises from uncertainties in the B lifetime and semileptonic branching ratio) below.

Figure 5 shows our predicted spectrum for $B^0 \to X_u^+ e^- \bar{\nu}_e$ where X_u^+ is a $u\bar{d}$ meson belonging to any of our eight lowest–lying meson families. (The spectrum for B^+ decay is almost identical: the splitting of the decay strength into neutral

isoscalar and isovector mesons has only a very small effect.) It is clear from our calculations that these low-lying states (which includeall states with $m_X \lesssim 1.7\,GeV$) do not in this case saturate the rate. One indication of this is that the $2S$ states still contribute as strongly as the $1S$ states. See Table II for details. Another is that our summed semileptonic rate is only about half of the free quark decay rate (also shown in Fig. 5). Recall, however, that our calculation does saturate the contributions of $B \to X_u e^- \bar{\nu}_e$ to the region at the end of the spectrum where $B \to X_c e^- \bar{\nu}_e$ is small or vanishes. This fraction of the spectrum is therefore all we need to determine (or to set an upper limit on) $|V_{ub}|$. Note that our $B \to X_u$ spectrum is considerably softer than the free quark spectrum.

Figure 6 shows our predicted B meson semileptonic spectra, boosted as is appropriate for $B\bar{B}$ pairs produced on the $\Upsilon(10575)$, compared to some recent data.[9,10]. Our absolute prediction of the shape of the spectrum with $V_{ub} = 0$ is in good agreement with experiment[7]. The implications of this observation, along with a discussion of its reliability, will be given in the next section.

IV. Discussion

Most attempts to extract $|V_{ub}|^2/|V_{cb}|^2$ from the $B \to X\, e\bar{\nu}$ endpoint spectrum have fit to the form (3) with $d\hat{\Gamma}$'s given by a QCD-perturbed free quark calculation in which extra parameters were introduced to correct for non-perturbative effects.[11]. With recent improvements in the data these attempts have, as might have been anticipated, encountered difficulties[7,9]. These difficulties have made it clear that the predicted endpoint behavior of the Ref. 11 calculations are being controlled almost entirely not by perturbative QCD, but by the *ad hoc* parameters introduced to describe bound state effects. Our calculation, in contrast, is especially suitable for the endpoint region: not only is the

dynamics of the quark model more appropriate to this region, but also it correctly handles the kinematics of the opening of new channels with their appropriate quantum numbers.

Of course our calculations still have sources of uncertainty. Nevertheless, we would first like to stress that our calculation of $B \to X_c\, e^- \overline{\nu}_e$ seems to be largely immune to these uncertainties. The success of the analogous $D \to X_s\, e^+ \nu_e$ calculation is evidence for the reliability of $B \to X_c\, e^- \overline{\nu}_e$, but we have also checked that reasonable variations of the wavefunctions (for example, ones that change r_f by 30%) have little effect on our spectra. There are some simple reasons for this. One is that the $b\overline{d}$ and $c\,\overline{d}$ wavefunctions are sufficiently similar that they overlap very well (see eqs. (11) and (12)). Another is that in the recoiling X_c the charm quark carries most of the momentum so that the calculation does not rely on the tail of the $B \to X_c$ form factor. Also, the recoiling X_c is not excessively relativistic. It is more difficult to assess the systematic uncertainties associated with this calculation. We will discuss below some possible improvements on our methods which could check several possible sources of error,but for now we just note that the success of our predictions for $K \to \pi$, $D \to X_s$, and various known features of $B \to X_c$, along with the demonstrably weak parameter dependence of our results, lead us to have confidence that the absolute rate predictions shown in Fig. 4 are valid at the 20% level, and that the shape of the predicted electron spectrum is very good.

For $B \to X_u e^- \overline{\nu}_e$ our predicted spectral shape is once again very stable in the endpoint region. However, we have considerably less confidence in this case in our ability to predict absolute rates: few of the features which stabilized $B \to X_c\, e^- \overline{\nu}_e$ are present here. for example, when we vary the β's over the range we consider reasonable, we get substantial variations in the absolute rates of the

exclusive modes. (The inclusive rate should be more stable, but recall that our calculation does not exhaust the exclusive modes). We have concluded that our absolute rate predictions in this case could be as much as 30% higher and a factor of two lower than the true rates. This uncertainty will affect our ability to determine (or bound) V_{ub} from the data.

There are, incidentally, two general approaches one can take to determine V_{ub}. One could use Fig. 6 alone to determine the fraction $|V_{ub}|^2/|V_{cb}|^2$ of the $B \to X_u$ spectrum which when added to the $B \to X_c$ spectrum leads to consistency with the data in the endpoint region. This method is weakened by the fact that our $B \to X_u$ spectra does not saturate the spectrum of $b \to u$ transitions. It is possible that a better determination of $|V_{ub}|^2$ can be made by using a "hybrid model" which requires free quark behavior of $\frac{d\hat{\Gamma}}{dx}$ for small x matching onto our spectrum near the endpoint $x = x_m$. One such model is

$$\frac{d\hat{\Gamma}}{dx} = 16\,x^2(3-4x)\left[\frac{1-x/x_m}{1-x/(x_m+\delta)}\right]^2 \hat{\Gamma}^{\text{free}} \tag{19}$$

where $\delta > 0$ is a parameter used to fit onto our endpoint spectrum. The main advantages of such a hybrid model are that it allows a global fit to the electron energy spectrum and that it only uses our prediction for the shape of the electron spectrum in the endpoint region which is much more reliable than its normalization. Of course in such a fit one must contend with uncertainties in $\hat{\Gamma}^{\text{free}}$ which are still substantial.

One might hope to reduce the uncertainties in the results we have presented by improving upon our quark model calculation. To a certain extent we believe that this is possible. It would be useful, for example, to extend our calculations to higher masses (see, however, the warning in our introduction). It would also

be interesting to check on the importance of relativistic effects[13]. Unfortunately, we doubt the utility of making a check of such effects in the bag model (though it naturally comes to mind as a relativistic quark model) since one will encounter two problems with the static bag approximation: heavy quark wavefunctions will not be adequately described, and the recoiling quark will populate both excited meson states and spurious center of mass motion states. An alternative is to build some relativistic corrections into the quark potential model[12]. Here one must be careful to ensure that the model predicts meson spectra and static properties as well as the non–relativistic quark model. One might also consider supplementing our quark model calculation with some sort of pole dominance model for the t–dependence of the weak form factors. Our form factors are actually quite close to pole dominance form factors in many cases, but we can also appreciate from our calculation that the pole model is not generally applicable. These form factors are largest (and therefore normally most important) at the zero recoil point where the quark model applies and where, in some cases, there is no reason to expect a single meson pole to dominate. An extreme case would be the elastic form factor of the η_c: this form factor near $t = 0$ will clearly be controlled by the η_c wavefunction (which will give $r_f \sim (m_c\,\alpha_s)^{-1}$) and not by the lowest vector meson (which would give $r_f \sim m_c^{-1}$). The failure of vector meson dominance in this case is easy to understand: on the scale of m_ψ^2, the spacing between vector meson states is small.

V. Conclusions and Summary

We have argued that the extraction of $|V_{ub}|^2/|V_{cb}|^2$ from the endpoint of $B \to X\, e^-\overline{\nu}_e$ requires an understanding of the non–perturbative physics which binds the quarks into hadrons. The quark model calculation presented here

represents one approach to this physics; we believe that it will be difficult at the moment to improve upon the resulting picture of the endpoint.

Our results give a $B \to X_c$ endpoint spectrum that is softer than the free quark spectrum; this leads to a predicted $B \to X_c$ spectrum that fits the data quite well with no admixture of $B \to X_u$. Our $B \to X_u$ spectrum is considerably softer than the free quark spectrum, so that the limits which one can obtain on the strength of V_{ub} from the lepton spectra in the endpoint region will be correspondingly weaker.

While improved measurements of the endpoint spectrum may well remain the best way to limit and eventually observe V_{ub}, our calculation does open up one other possible avenue. Since we provide absolute rates for a large number of *exclusive* semileptonic modes to non–charmed mesons (see Table II), a limit on (or a measurement of) any of these modes can now be turned into a limit on (or a measurement of) $|V_{ub}|$.

We also note that as a byproduct of these calculations we have made predictions for how the $B \to X_c$, $B \to X_u$, $D \to X_s$, and $D \to X_d$ spectra are built up out of exclusive channels[14]. These predictions, which are of interest in their own right, can be used to check the reliability of our calculations. It would be especially rigorous to check our predictions (via α,β_{++}, and γ) of the detailed structure of the relevant Dalitz plots. One other possible application of these results would be to use our predictions to extract V_{cd} from an exclusive mode like $D^+ \to \rho^0 e^+ \nu_e$, thereby producing an independent check on the validity of the K–M parameterization.

Acknowledgements

This research was supported in part by grants from the Natural Sciences and Engineering Research Council of Canada and by D.O.E. grants under contracts DEAC03–81–ER40051 and DE–FG03–84ER40172. M.B.W. also was supported by an Alfred P. Sloan Foundation Fellowship.

References

1. M. Kobayashi and T. Maskawa, Prog. Theor. Phys. 49, 652 (1973).
2. See, e.g., N. Isgur in Particles and Fields – 1981: Testing the Standard Model, Proceedings of the Meeting of the Div. of Particles and Fields of the APS, Santa Cruz, California, ed. by C. Heusch and W. T. Kirk. (AIP, New York, 1982) p. 1.
3. N. Isgur, Phys. Rev. D12, 3666 (1975).
4. C. Hayne and N. Isgur, Phys. Rev. D25, 1944 (1982);
   N. Isgur, Acta. Phys. Pol. B6, 1081 (1977).
5. M. Ademollo and R. Gatto, Phys. Rev. Lett. 13, 264 (1964).
6. D. M. Coffman (representing the Mark III collaboration), in Hadron Spectroscopy – 1985, AIP Conf. Proc. 132: the Int. Conf. on Hadron Spectroscopy, College Park, Maryland, edited by S. Oneda (AIP, New York, 1985) p. 322.
7. E. H. Thorndike, at the International Symposium on Lepton and Photon Interactions, Kyoto, 1985;
   T. Bowcock, *et al.*, (CLEO collaboration); paper submitted to this conference.
8. W. Bacino, *et al.*, Phys. Rev. Lett. 43, 1073 (1979).
9. S. Stone, in Proceedings of the 1983 International Symposium on Lepton and Photon Interactions at High Energies, Ithaca, New York, 1983, ed. by D. G. Cassel and D. L. Kreineck, (Cornell University, 1983) p. 203.
10. H. Schröder (representing the ARGUS collaboration) in Hadron Spectroscopy – 1985, AIP Conf. Proc. 132: the Int. Conf. on Hadron Spectroscopy, College Park, Maryland, ed. by S. Oneda (AIP, New York, 1985) p. 368. In addition to the data shown in Fig. 6 the CUSB collaboration (C. Klopfenstein *et al.*, Phys. Lett. 130B, 444 1983) has also measured the electron spectrum.

11. G. Altarelli, *et al.*, Nucl Phys. B208, 365 (1982).

12. For a recent general discussion see S. Godfrey and N. Isgur, Phys. Rev. D32, 189 (1985). The $^1S_0 \to {}^1S_0$ transitions have been considered in a relativistic context by S. Godfrey, Univ. of Toronto preprint 1984, TRIUMF preprint, 1985.

13. One empirical check would be to determine whether the a_+ amplitudes in $D \to K^*$ and $B \to D^*$ are negligible (see Appendix).

14. For some other recent discussions of exclusive modes see F. E. Close, G. J. Gounaris, and J. E. Paschalis, Phys. Lett. 149B, 209 (1984); M. Suzuki, U. C. Berkeley preprint UCB–PTH–85/12, 1985.

Appendix: Formulas for the Functions α, β_{++} and γ in $B^0 \to X^+ e^- \overline{\nu}_e$

We give here the formulas for α, β_{++}, and γ required in eq. (8) for $\frac{d^2\Gamma}{dx\,dy}$ for $X = q\overline{d}$ in the states 1^1S_0, 1^3S_1, 1^3P_2, 1^3P_1, 1^3P_0, 1^1P_1, 2^1S_0, and 2^3S_1 in the spectroscopic notation $n^{2S+1}L_J$. Throughout the following we will employ the definitions

$$\mathbf{F}_n = \left[\frac{\tilde{m}_X}{\tilde{m}_B}\right]^{1/2} \left[\frac{\beta_B\,\beta_X}{\beta_{BX}^2}\right]^{n/2} \exp\left\{-\left[\frac{m_d^2}{4\tilde{m}_X\,\tilde{m}_B}\right]\frac{(t_m - t)}{\beta_{BX}^2}\right\} \tag{A1}$$

where

$$\beta_{BX}^2 = \frac{1}{2}(\beta_B^2 + \beta_X^2) \tag{A2}$$

and

$$t_m = (m_B - m_X)^2\,, \tag{A3}$$

is the maximum momentum transfer, and

$$\mu_\pm = (m_q^{-1} \pm m_b^{-1})^{-1}. \tag{A4}$$

We also denote by V_μ and A_μ the quark currents $\overline{q}\,\gamma_\mu\,b$ and $\overline{q}\,\gamma_\mu\gamma_5\,b$ respectively.

The determination of most of the form factors given below is based on a straightforward application of the discussion of the text. However, some of the form factors we need (those corresponding to X recoiling with non–minimal orbital angular momentum) require for their complete specification knowledge of the quark currents and boosted state vectors beyond leading order in v/c. In such cases we show below all terms which are expected to be more important than those we are unable to calculate, and denote the pieces we are thereby

ignoring in our computations by an additional term: $+O(\cdots)$. Since the contributions of these incompletely determined higher order form factors vanish at the threshold $\vec{p}_X = 0$, this uncertainty should not introduce a large error in our computed rates.

a) 1^1S_0

The axial vector matrix element vanishes, and with

$$\langle X(p_X) | V_\mu | B(p_B) \rangle \equiv f_+(p_B + p_X)_\mu + f_-(p_B - p_X)_\mu \tag{A5}$$

we obtain

$$\alpha = \gamma = 0 \tag{A6}$$

and

$$\beta_{++} = f_+^2 , \tag{A7}$$

where

$$f_+ = \mathbf{F}_3 \left[1 + \frac{m_b}{2\mu_-} - \frac{m_b m_q}{4\mu_+\mu_-} \frac{m_d}{\tilde{m}_X} \frac{\beta_B^2}{\beta_{BX}^2} \right] \tag{A8}$$

and

$$f_- = \mathbf{F}_3 \left[1 - (\tilde{m}_B + \tilde{m}_X)\left(\frac{1}{2m_q} - \frac{1}{4\mu_+} \frac{m_d}{\tilde{m}_X} \frac{\beta_B^2}{\beta_{BX}^2} \right) \right] \tag{A9}$$

b) 1^3S_1

With

$$\langle X(p_X,\varepsilon)\,|A_\mu|\,B(p_B)\rangle \equiv f\varepsilon_\mu^* + a_+(\varepsilon^*\cdot p_B)(p_B+p_X)_\mu + a_-(\varepsilon^*\cdot p_B)(p_B-p_X)_\mu \tag{A10}$$

and

$$\langle X(p_X,\varepsilon)\,|\,V_\mu\,|\,B(p_B)\rangle \equiv ig\,\varepsilon_{\mu\nu\rho\sigma}\varepsilon^{*\nu}(p_B+p_X)^\rho(p_B-p_X)^\sigma\,. \tag{A11}$$

we have

$$\alpha = f^2 + 4m_B^2\vec{p}_X^{\,2}g^2 \tag{A12}$$

$$\beta_{++} = \frac{1}{4}\frac{f^2}{m_X^2} - m_B^2 y\,g^2 + \frac{1}{2}\left[\frac{m_B^2}{m_X^2}(1-y)-1\right]fa_+ + \frac{m_B^2\vec{p}_X^{\,2}}{m_X^2}a_+^2 \tag{A13}$$

and

$$\gamma = 2gf\,. \tag{A14}$$

Here $\vec{p}_X^{\,2} = ([m_B^2(1-y)+m_X^2]^2/4m_B^2) - m_X^2$ is the square of the recoil three momentum of the X. The form factors f and g are given by

$$f = 2\tilde{m}_B\,\mathbf{F}_3 \tag{A15}$$

$$g = \mathbf{F}_3\frac{1}{2}\left[\frac{1}{m_q} - \frac{1}{2\mu_-}\frac{m_d}{\tilde{m}_X}\frac{\beta_B^2}{\beta_{BX}^2}\right]. \tag{A16}$$

The form factor a_+ is of the troublesome type described above. In this case there are no calculable contributions which are expected to dominate the recoil uncertainties, and we can only calculate that $a_+ = O(\frac{f}{\tilde{m}_B\,\tilde{m}_X})$.

c) 1^3P_2

With

$$\left\langle X(p_X,\varepsilon)\,|\,V_\mu\,|\,B(p_B)\right\rangle \equiv ih\,\varepsilon_{\mu\nu\lambda\rho}\varepsilon^{\nu\alpha^*}\,p_{B\alpha}(p_B+p_X)^\lambda(p_B-p_X)^\rho \qquad \text{(A17)}$$

and

$$\left\langle X(p_X,\varepsilon)\,|A_\mu|\,B(p_B)\right\rangle \equiv k\,\varepsilon^*_{\mu\nu}p_B^\nu + b_+(\varepsilon^*_{\alpha\beta}p_B^\beta p_B^\beta)(p_B+p_X)_\mu$$

$$+\,b_-(\varepsilon^*_{\alpha\beta}p_B^\beta p_B^\beta)(p_B-p_X)_\mu\,, \qquad \text{(A18)}$$

we have

$$\alpha = \frac{1}{2}\frac{m_B^2\vec{p}_X^{\,2}}{m_X^2}(k^2+4m_B^2\vec{p}_X^{\,2}h^2)\,, \qquad \text{(A19)}$$

$$\beta_{++} = -\frac{1}{2}y\,\frac{m_B^4\vec{p}_X^{\,2}}{m_X^2}h^2 + \frac{m_B^2}{24m_X^2}[y+\frac{4\vec{p}_X^{\,2}}{m_X^2}]k^2$$

$$+\frac{2}{3}\left[\frac{m_B^2\vec{p}_X^{\,2}}{m_X^2}\right]^2 b_+^2 + \frac{1}{3}\frac{m_B^2\vec{p}_X^{\,2}}{m_X^2}[\frac{m_B^2}{m_X^2}(1-y)-1]k\,b_+\,, \qquad \text{(A20)}$$

and

$$\gamma = \frac{m_B^2\vec{p}_X^{\,2}}{m_X^2}kh\,. \qquad \text{(A21)}$$

The form factors h and k are given by

$$h = \mathbf{F}_5\frac{m_d}{2\sqrt{2}\,\tilde{m}_B\beta_B}\left[\frac{1}{m_q}-\frac{m_d}{2\tilde{m}_X\mu_-}\frac{\beta_B^2}{\beta_{BX}^2}\right], \qquad \text{(A22)}$$

$$k = \sqrt{2}\,\mathbf{F}_5\frac{m_d}{\beta_B}\,. \qquad \text{(A23)}$$

The form factor b_+, is like a_+ in $^3S_1$ decays: we can only conclude that $b_+ = O(\frac{k}{\tilde{m}_B \tilde{m}_X})$.

d) 1^3P_1

The relevant matrix elements are

$$\langle X(p_X,\varepsilon)\,|V_\mu|\,B(p_B)\rangle \equiv l\,\varepsilon_\mu^* + c_+(\varepsilon^*\cdot p_B)(p_B+p_X)_\mu + c_-(\varepsilon^*\cdot p_B)(p_B-p_X)_\mu \tag{A24}$$

and

$$\langle X(p_X,\varepsilon)\,|A_\mu|\,B(p_B)\rangle \equiv i\,q\,\varepsilon_{\mu\nu\rho\sigma}\varepsilon^{\nu *}(p_B+p_X)^\rho(p_B-p_X)^\sigma\,. \tag{A25}$$

It follows that

$$\alpha = l^2 + 4m_B^2\vec{p}_X^{\,2}q^2 \tag{A26}$$

$$\beta_{++} = l^2/4m_X^2 - m_B^2 y\,q^2 + \frac{1}{2}\left[\frac{m_B^2}{m_X^2}(1-y)-1\right]lc_+ + \frac{m_B^2\vec{p}_X^{\,2}}{m_X^2}c_+^2 \tag{A27}$$

$$\gamma = 2ql\,, \tag{A28}$$

where

$$q = \frac{1}{2}F_5\frac{m_d}{\tilde{m}_X}\frac{1}{\beta_B}\,, \tag{A29}$$

$$l = -\mathbf{F}_5 \tilde{m}_B \beta_B \left[\frac{1}{\mu_-} + \frac{1}{2} \frac{m_d}{\tilde{m}_X} \frac{(t_m - t)}{\beta_B^2} \left(\frac{1}{m_q} - \frac{1}{2\mu_-} \frac{m_d}{\tilde{m}_X} \frac{\beta_B^2}{\beta_{BX}^2} \right) \right]$$

and

$$c_+ = \mathbf{F}_5 \frac{m_d m_b}{4\beta_B \tilde{m}_B} \left[\frac{1}{\mu_-} - \frac{m_d m_q}{2\tilde{m}_X \mu_-^2} \frac{\beta_B^2}{\beta_{BX}^2} + \frac{2\beta_B^2}{m_d m_b \mu_-} \right.$$

$$\left. + \left(\frac{1}{m_q} - \frac{m_d}{2\tilde{m}_X \mu_+} \frac{\beta_B^2}{\beta_{BX}^2} \right) \frac{(t_m - t)}{m_b \tilde{m}_B} \right] + O\left(\frac{l}{\tilde{m}_B \tilde{m}_X} \right). \tag{A31}$$

e) 1^3P_0

The vector matrix element vanishes, and with

$$\langle X(p_X) | A_\mu | B(p_B) \rangle \equiv u_+ (p_B + p_X)_\mu + u_- (p_B - p_X)_\mu \,, \tag{A32}$$

we have

$$\beta_{++} = u_+^2 \,, \tag{A33}$$

$$\alpha = \gamma = 0 \,, \tag{A34}$$

where

$$u_+ = \mathbf{F}_5 \frac{\beta_B}{\sqrt{6}} \left[\frac{m_d m_q m_b}{\beta_B^2 \tilde{m}_X \mu_-} + \frac{3}{2\mu_+} + \frac{m_d}{2\tilde{m}_B} \frac{(t_m - t)}{\beta_B^2} \right.$$

$$\left. \cdot \left(\frac{1}{m_q} - \frac{1}{2\mu_+} \frac{m_d}{\tilde{m}_X} \frac{\beta_B^2}{\beta_{BX}^2} \right) \right]. \tag{A35}$$

f) 1^1P_1

The matrix elements of the vector and axial vector currents have the form

$$\left\langle X(p_X,\varepsilon)\,|\,V_\mu\,|\,B(p_B)\right\rangle \equiv r\,\varepsilon_\mu^* + s_+(\varepsilon^*\cdot p_B)(p_B+p_X)_\mu + s_-(\varepsilon^*\cdot p_B)(p_B-p_X)_\mu \tag{A36}$$

and

$$\left\langle X(p_X,\varepsilon)\,|\,A_\mu\,|\,B(p_B)\right\rangle \equiv i\upsilon\,\varepsilon_{\mu\nu\rho\sigma}\varepsilon^{\nu*}(p_B+p_X)^\rho(p_B-p_X)^\sigma\,. \tag{A37}$$

It follows that

$$\alpha = r^2 + 4m_B^2\vec{p}_X^{\,2}\upsilon^2 \tag{A38}$$

$$\beta_{++} = r^2/4m_X^2 - m_B^2 y\,\upsilon^2 + \frac{1}{2}\left[\frac{m_B^2}{m_X^2}(1-y)-1\right]r\,s_+ + \frac{m_B^2\vec{p}_X^{\,2}}{m_X^2}s_+^2 \tag{A39}$$

$$\gamma = 2r\upsilon\,, \tag{A40}$$

with

$$\upsilon = 0 \tag{A41}$$

$$r = \mathbf{F}_5\frac{\tilde{m}_B\,\beta_B}{\sqrt{2}\,\mu_+} \tag{A42}$$

$$s_+ = \mathbf{F}_5\frac{m_d}{\sqrt{2}\,\beta_B\,\tilde{m}_B}\left[1+\frac{\beta_B^2}{2m_d\mu_+}+\frac{m_b}{2\mu_-}-\frac{m_b m_q}{4\mu_+\mu_-}\frac{m_d}{\tilde{m}_X}\frac{\beta_B^2}{\beta_{BX}^2}\right]+O\left[\frac{r}{\tilde{m}_X\tilde{m}_B}\right]. \tag{A43}$$

g) 2^1S_0

Again the axial contribution vanishes, and with

$$\langle X(p_X)\,|\,V_\mu\,|\,B(p_B)\rangle \equiv f'_+(p_B + p_X)_\mu + f'_-(p_B - p_X)_\mu\,, \tag{A44}$$

we have that

$$\alpha = \gamma = 0 \tag{A45}$$

$$\beta_{++} = f'^2_+\,. \tag{A46}$$

The form factor f'_+ is given by

$$f'_+ = \mathrm{F}_3\sqrt{3/8}\frac{m_b}{\mu_+}\left[\frac{\beta_B^2 - \beta_X^2}{\beta_B^2 + \beta_X^2} + \frac{m_q}{3\mu_-}\frac{m_d}{\tilde{m}_X}\frac{\beta_B^2}{\beta_{BX}^2}\left[\frac{7\beta_X^2 - 3\beta_B^2}{4\beta_{BX}^2}\right]\right.$$

$$\left. + \frac{1}{6}\frac{m_d}{\tilde{m}_X\tilde{m}_B}\frac{\beta_X^2}{\beta_{BX}^2}\frac{(t_m - t)}{\beta_{BX}^2}\left[1 - \frac{m_q}{2\mu_-}\frac{m_d}{\tilde{m}_X}\frac{\beta_B^2}{\beta_{BX}^2}\right]\right]. \tag{A47}$$

h) 2^3S_1

The matrix elements of the axial vector and vector currents can be written as

$$\langle X(p_X,\varepsilon)\,|\,A_\mu\,|\,B(p_B)\rangle \equiv f'\varepsilon^*_\mu + \alpha'_+(\varepsilon^*\cdot p_B)(p_B + p_X)_\mu$$

$$+ \alpha'_-(\varepsilon^*\cdot p_B)(p_B - p_X)_\mu \tag{A48}$$

and

$$\langle X(p_X,\varepsilon)\,|\,V_\mu\,|\,B(p_B)\rangle \equiv ig'\,\varepsilon_{\mu\nu\rho\sigma}\varepsilon^{\nu*}(p_B + p_X)^\rho(p_B - p_X)^\sigma\,. \tag{A49}$$

Then we find that

$$\alpha = f'^2 + 4m_B^2 \vec{p}_X^{\,2} g'^2 \tag{A50}$$

$$\beta_{++} = f'^2/4m_X^2 - m_B^2 y\, g'^2 + \frac{1}{2}\left[\frac{m_B^2}{m_X^2}(1-y) - 1\right] f' a'_+ + \frac{m_B^2 \vec{p}_X^{\,2}}{m_X^2} a'^2_+ \tag{A51}$$

$$\gamma = 2g'f' \,. \tag{A52}$$

The form factors f' and g' are given by

$$f' = \mathbf{F}_3 \sqrt{6}\, \tilde{m}_B \left[\frac{\beta_B^2 - \beta_X^2}{\beta_B^2 + \beta_X^2} \frac{1}{6} \frac{m_d^2}{\tilde{m}_X \tilde{m}_B} \frac{\beta_X^2}{\beta_{BX}^2} \frac{(t_m - t)}{\beta_{BX}^2}\right] \tag{A53}$$

$$g' = \mathbf{F}_3 \sqrt{\frac{3}{8}} \left[\left(\frac{\beta_B^2 - \beta_X^2}{\beta_B^2 + \beta_X^2} + \frac{1}{6} \frac{m_d^2}{\tilde{m}_X \tilde{m}_B} \frac{\beta_X^2}{\beta_{BX}^2} \frac{(t_m - t)}{\beta_{BX}^2}\right)\left[\frac{1}{m_q} - \frac{m_d}{3\mu \tilde{m}_X} \frac{\beta_B^2}{\beta_{BX}^2}\right] + \frac{m_d}{3\mu_- \tilde{m}_X} \frac{\beta_B^2 \beta_X^2}{\beta_{BX}^4}\right] . \tag{A54}$$

The form factor a'_+, like a_+, undetermined: we can only conclude that $a'_+ = 0\,(\frac{f'}{\tilde{m}_B \tilde{m}_X})$.

Table I: Variational Solutions of the Coulomb plus Linear Problem*

meson flavor:	$u\bar{d}$	$u\bar{s}$	$u\bar{c}$	$u\bar{b}$
$\beta_S(GeV)$	0.31	0.34	0.39	0.41
θ	-- negligible --			
$\beta_P(GeV)$	0.27	0.30	0.34	–

* In general ψ^{1S} and ψ^{2S} mix with some mixing angle θ so that the ground state wavefunction is $\cos\theta\,\psi^{1S} + \sin\theta\,\psi^{2S}$. For the particular masses and potentials in these systems, θ turns out to always be less than 0.01.

Table II: Partial Decay Rates for $B^0 \to X_u^+ e^-\overline{\nu}_e$ in units of $|V_{ub}|^2 \times 10^{14}\, sec^{-1}$

X_u^+	$\Gamma(B^0 \to X_u^+ e^-\overline{\nu}_e)$
π	.02
ρ	.16
$A_2+A_1+A_0+B$	.19
$\pi'+\rho'$	.20

Figure Captions

1. $\frac{1}{\Gamma}\frac{d\Gamma}{dE_e}$ for $D \to X_s e^+ \nu_e$ showing the contributions of K, K^*, and the total contribution from all 1S, 1P and 2S states; also shown is the corresponding free quark curve. Absolute rates can be obtained by using $\Gamma = 0.21 \times 10^{12} sec^{-1}$ and $\Gamma^{free} = 0.34 \times 10^{12} sec^{-1}$.

2. $d\Gamma/dE_e$ for $D \to X_s e^+ \nu_e$ from Fig. 1 boosted to correspond to D's from $\psi(3770)$ decay and compared to the data of Ref. 8. The integrated theoretical and experimental rates have been roughly adjusted to agree in order to facilitate a comparison of the spectral shapes.

3. $\frac{1}{\Gamma}\frac{d\Gamma}{dE_e}$ for $D \to X_d e^+ \nu_e$ showing the contributions of π,ρ and the total contribution from all 1S, 1P and 2S states; also shown is the corresponding free quark curve. Absolute rates can be obtained by using $\Gamma = 0.25 \times 10^{12} |V_{cd}|^2 sec^{-1}$ and $\Gamma^{free} = 0.54 \times 10^{12} |V_{cd}|^2 sec^{-1}$.

4. $\frac{1}{\Gamma}\frac{d\Gamma}{dE_e}$ for $B \to X_c e^- \overline{\nu}_e$ showing the contributions of D,D^* and the total contributions from 1S, 1P and 2S states; also shown is the corresponding free quark curve. Absolute rates can be obtained by using $\Gamma = 0.58 \times 10^{14} |V_{cb}|^2 sec^{-1}$ and $\Gamma^{free} = 0.49 \times 10^{14} |V_{cb}|^2 sec^{-1}$.

5. $\frac{1}{\Gamma^{free}}\frac{d\Gamma}{dE_e}$ for $B \to X_u^+ e^- \overline{\nu}_e$ showing the contributions of π,ρ, the 1P states A_2,A_1,A_0 and B, and the 2S states π' and ρ'; also shown is the free quark curve $\frac{1}{\Gamma^{free}}\frac{d\Gamma^{free}}{dE_e}$. Absolute rates can be obtained by using $\Gamma^{free} = 1.18 \times 10^{14} |V_{ub}|^2 sec^{-1}$.

6. $d\Gamma/dE_e$ for $B \to X_c e^- \overline{\nu}_e$ and $B \to X_u e^- \overline{\nu}_e$ from Figs. 4 and 5 boosted to correspond to B's from $\Upsilon(10575)$ decay and compared to the shape of the spectra of Refs. 9 and 10. The two curves are correctly normalized to one another for $|V_{cb}| = |V_{ub}|$; the data sets are normalized to fit the $B \to X_c e^- \overline{\nu}_e$ curve.

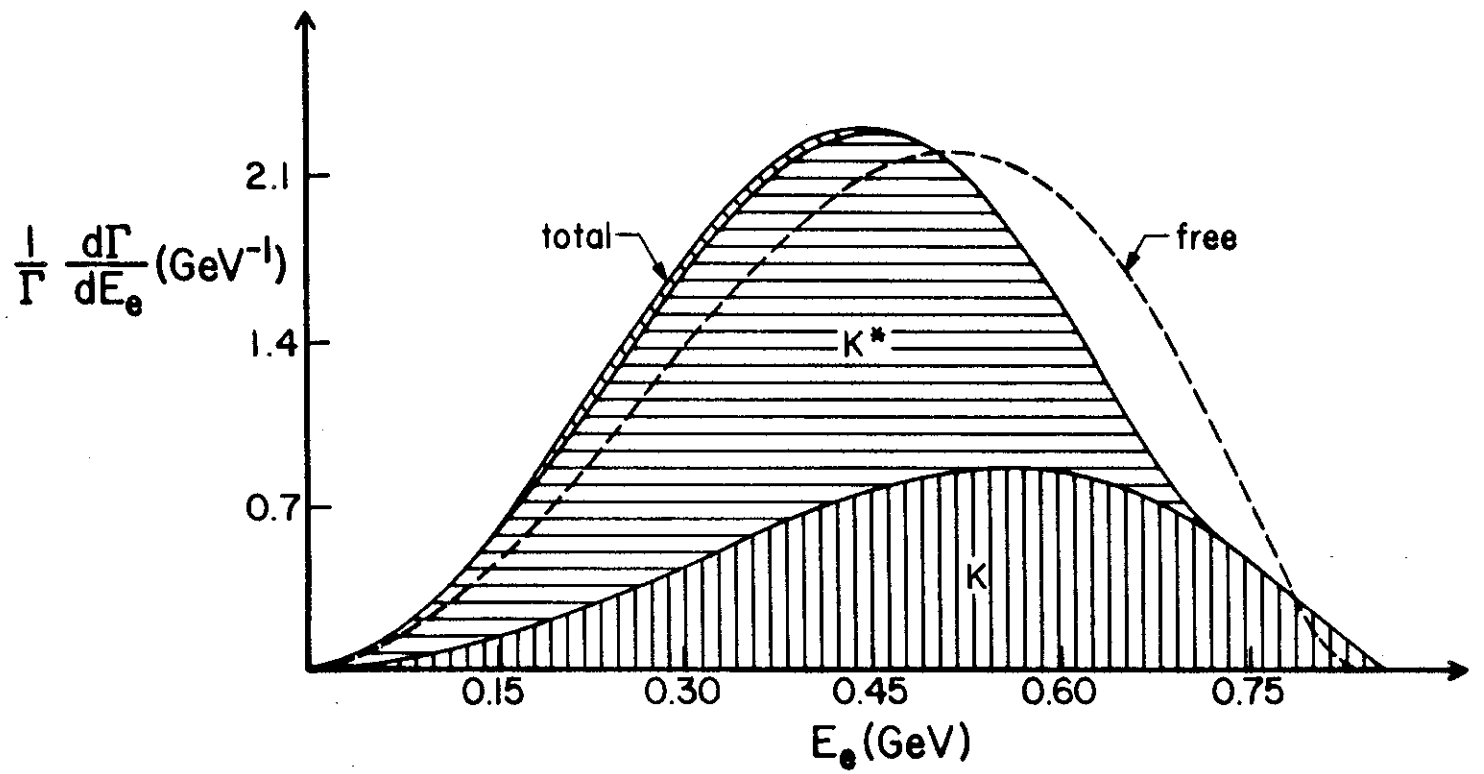
$\frac{1}{\Gamma}\frac{d\Gamma}{dE_e}(GeV^{-1})$
2.1
1.4
0.7
total
free
K*
K
0.15
0.30
0.45
0.60
0.75
E_e (GeV)

FIGURE 1

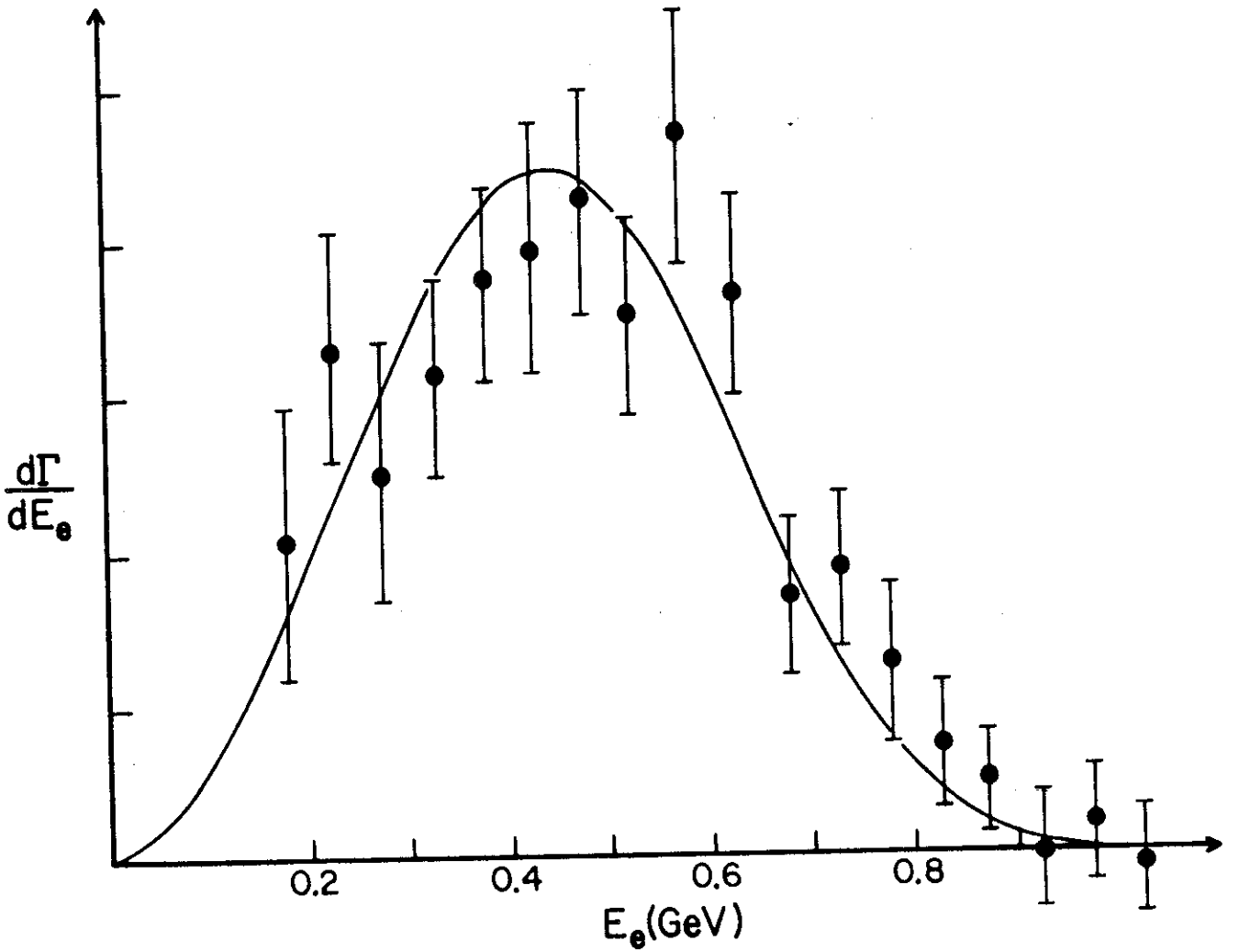

FIGURE 2

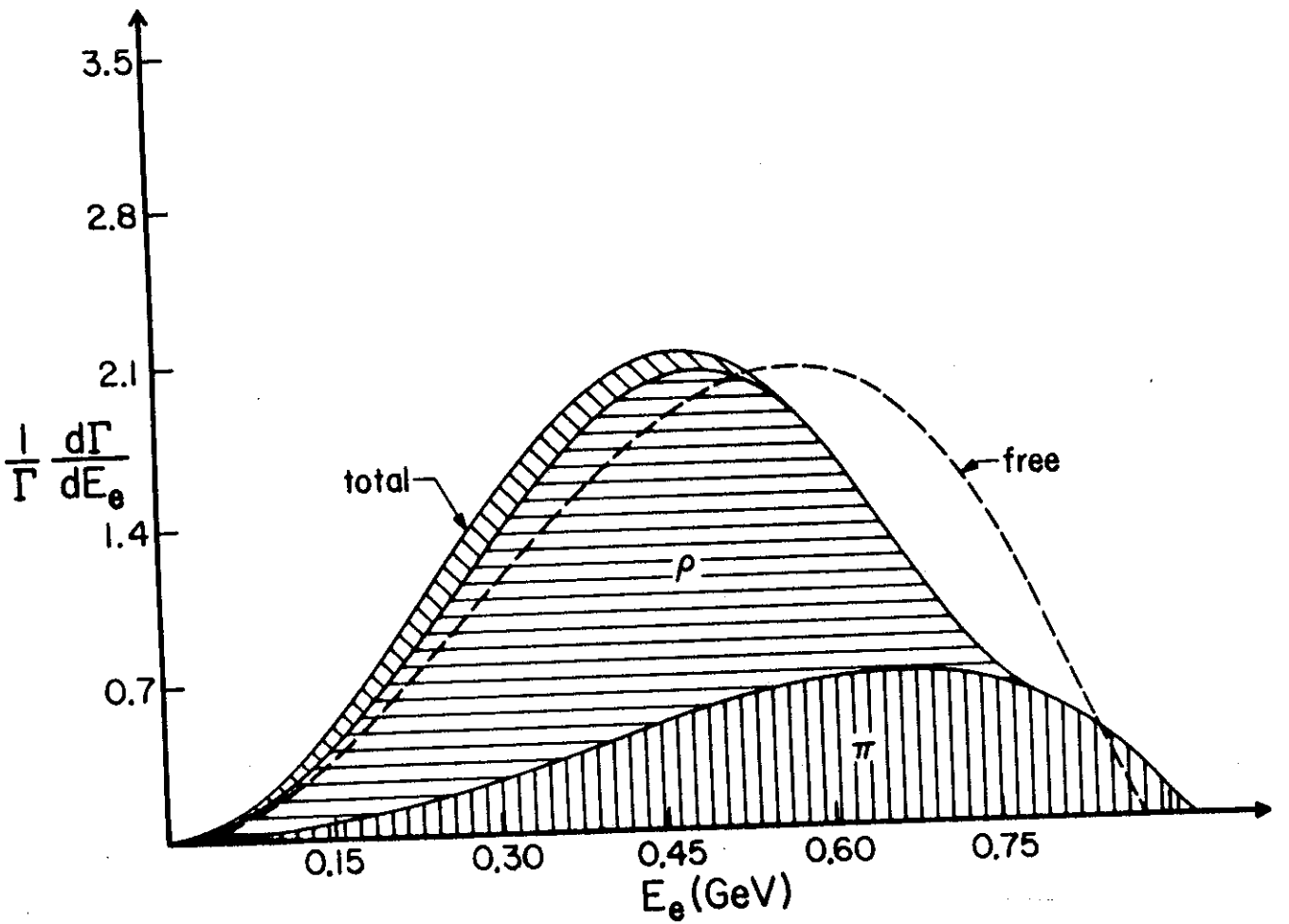
3.5
2.8
2.1
1.4
0.7
$\frac{1}{\Gamma}\frac{d\Gamma}{dE_e}$
total
free
ρ
π
0.15
0.30
0.45
0.60
0.75
E_e(GeV)

FIGURE 3

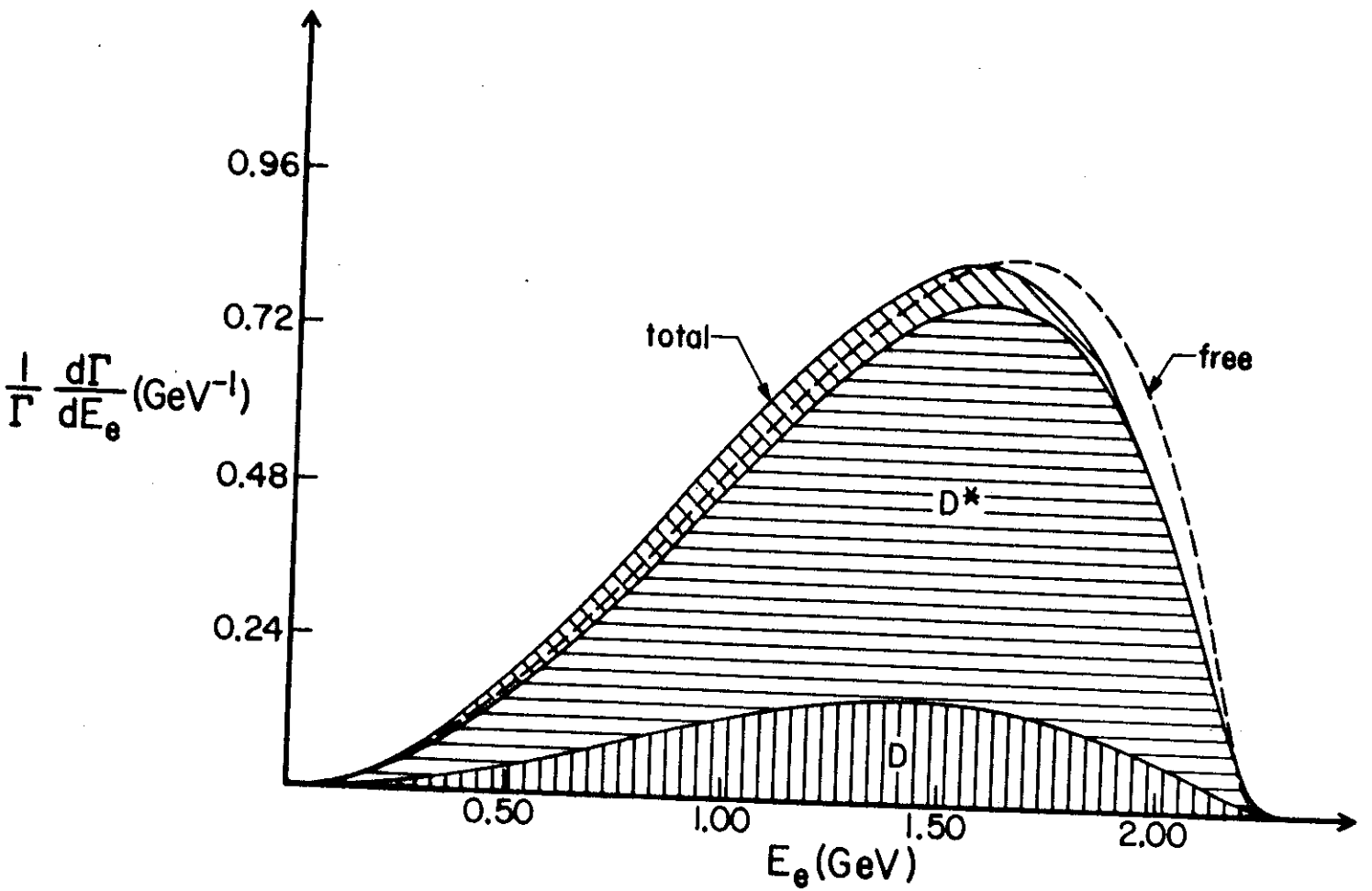
0.96
0.72
0.48
0.24
$\frac{1}{\Gamma}\frac{d\Gamma}{dE_e}(GeV^{-1})$
total
free
D*
D
0.50
1.00
1.50
2.00
$E_e(GeV)$

FIGURE 4

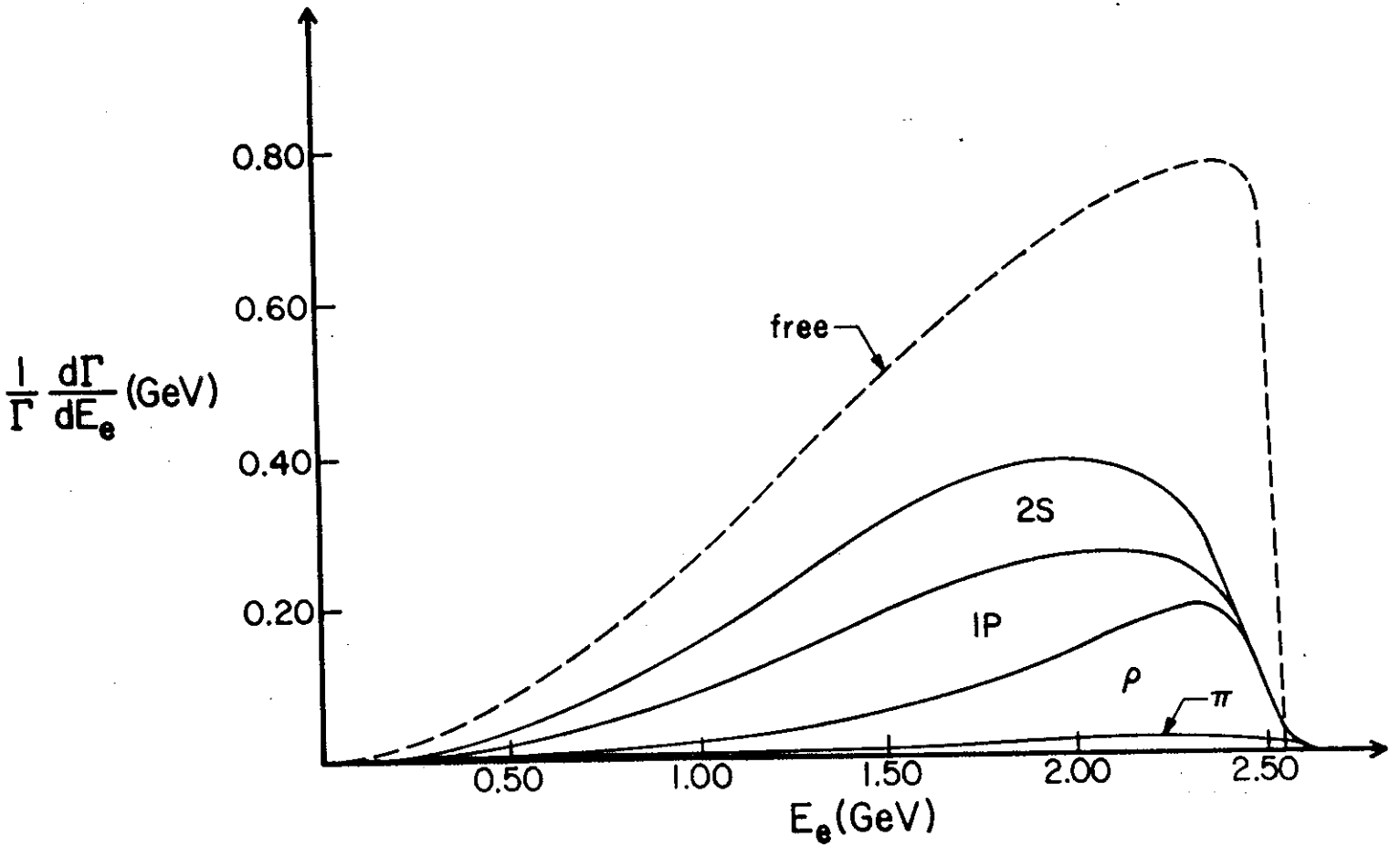
$\frac{1}{\Gamma}\frac{d\Gamma}{dE_e}$ (GeV)
0.80
0.60
0.40
0.20
free
2S
1P
ρ
π
0.50
1.00
1.50
2.00
2.50
E_e(GeV)

FIGURE 5

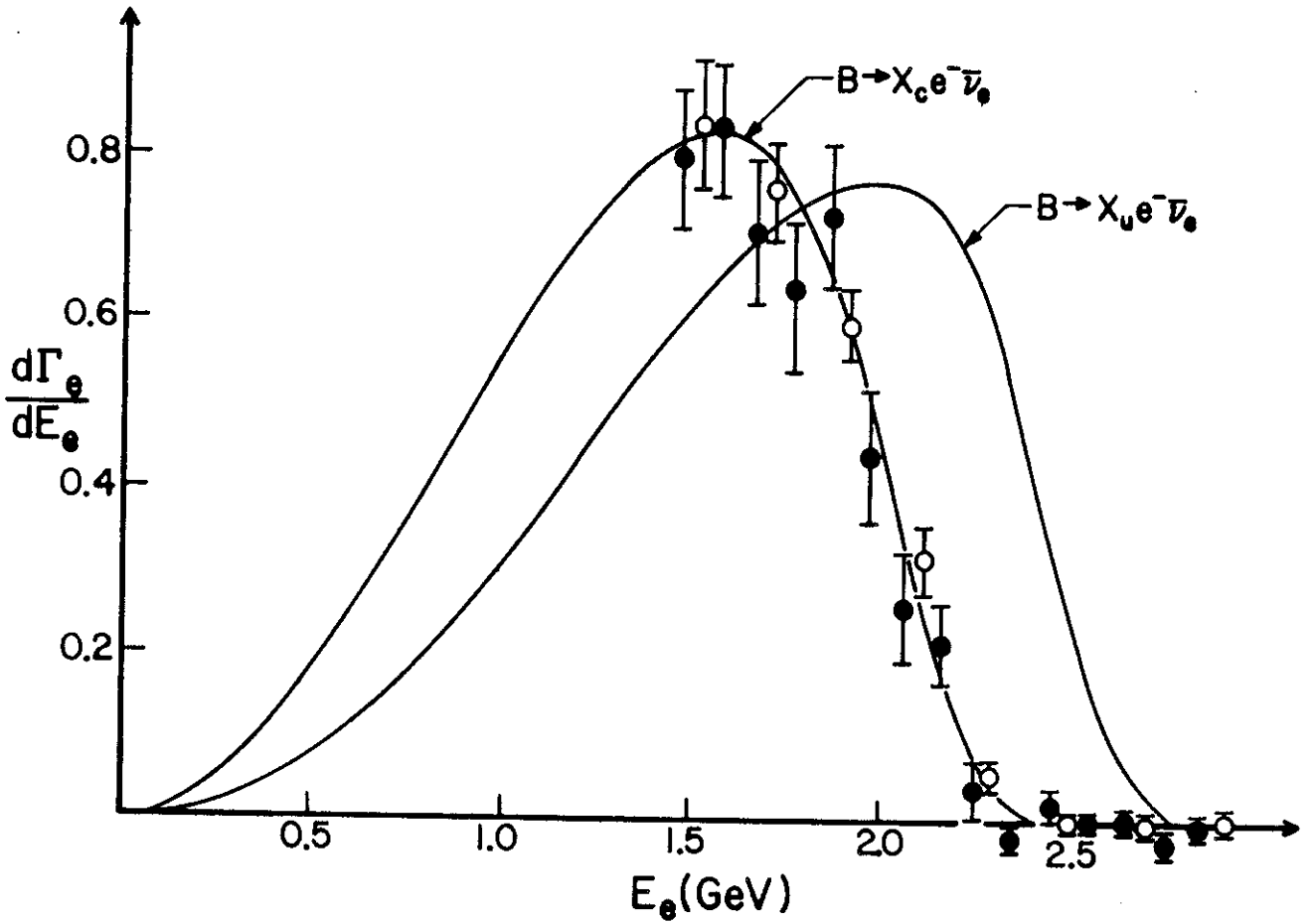

FIGURE 6